Memory effects from topological connectivity of nematic liquid crystals confined in porous materials

Takeaki ARAKI[a,b], Marco BUSCAGLIA[c], Tommaso BELLINI[c] and Hajime TANAKA[a]

a) Institute of Industrial Science, University of Tokyo, Japan
b) Department of Physics, Kyoto University, Japan
c) Department of Chemistry, Biochemistry and Biotecnology, University of Milano, Italy

Liquid crystal

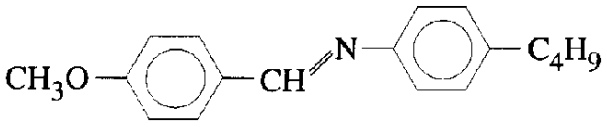

n-4'-MethoxyBenzylidene-n-ButylAnilin (MBBA)

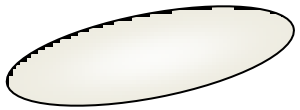

Liquid crystals are substances that exhibit a phase of matter that has properties between those of a conventional liquid, and those of a solid crystal.

smectic

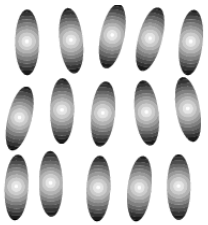

orientational order and layering

nematic

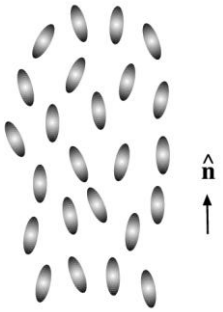

orientational order

isotropic

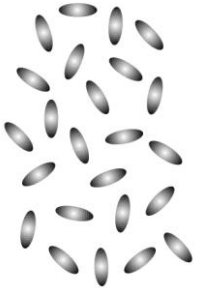

disorder (Liquid phase)

temperature

Elasticity of nematic phase

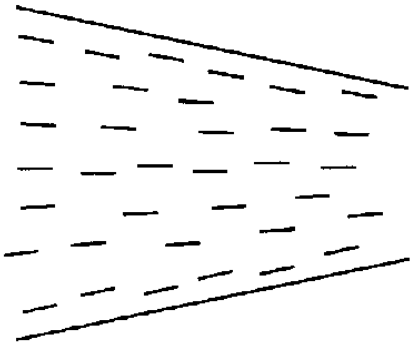

spray (K_1)

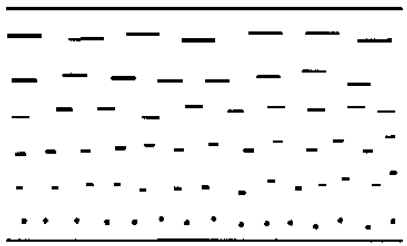

twist (K_2)

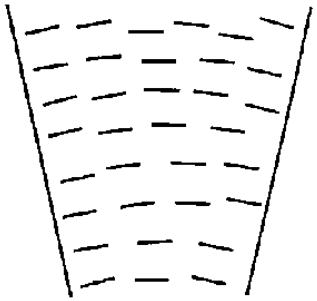

bend (K_3)

Frank elastic energy

$$F = \int d\vec{r}\left[\frac{1}{2}\{K_1(\vec{\nabla}\cdot\hat{n})^2 + K_2(\hat{n}\cdot(\vec{\nabla}\times\hat{n}))^2 + K_3(\hat{n}\times(\vec{\nabla}\times\hat{n}))^2\right]$$

$\vec{n}(\vec{r})$ local director field $(|\vec{n}|=1)$

Defects in liquid crystals

When incommensurate domains contact, defects are formed at the domain boundary

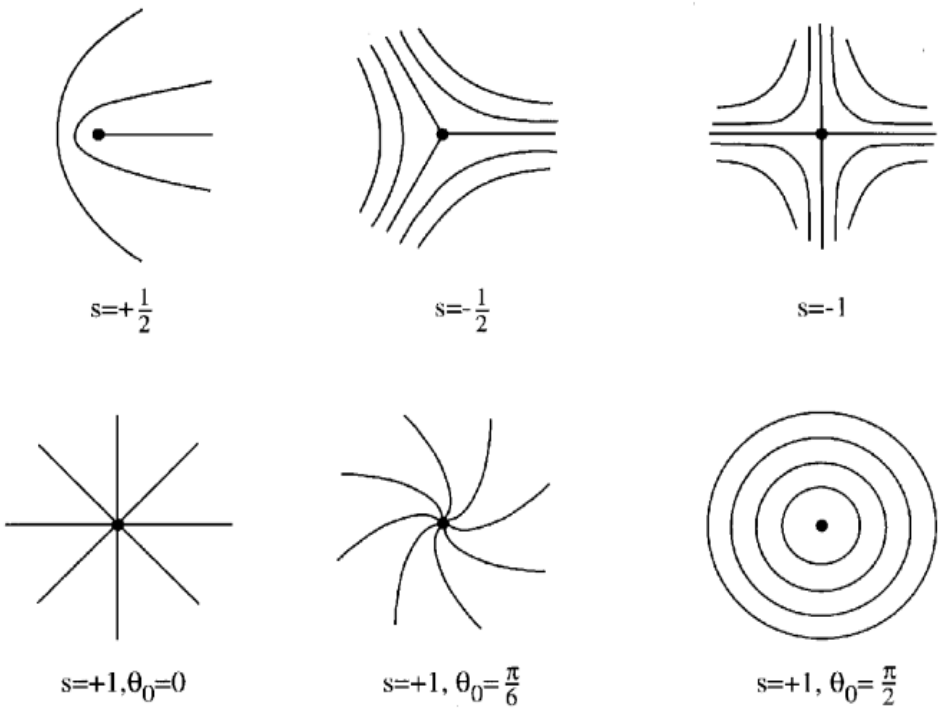

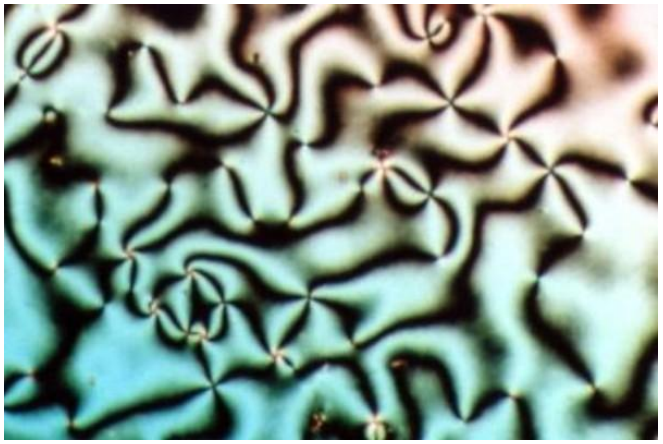

Schlieren texture

$$\phi(\vec{r}) = s\theta(\vec{r}) + \theta_0$$

θ : angular coordinate
ϕ: angle of director field
s: the strength of the defect

defect core energy $E_d = \frac{1}{K}\int d\vec{r}\left(\nabla\phi\right)^2 \propto s^2$

Defects in liquid crystals

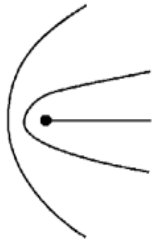

$s=+\frac{1}{2}$

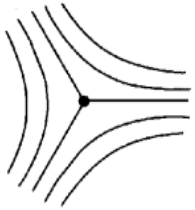

$s=-\frac{1}{2}$

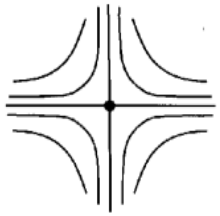

$s=-1$

A defect of *s* interacts with that of *s'*.
Roughly, the strength of the interaction is proportional to *ss'*.

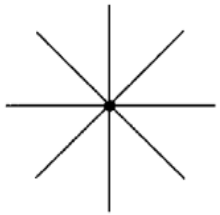

$s=+1, \theta_0=0$

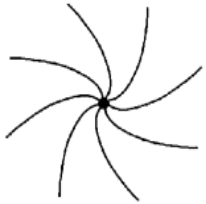

$s=+1, \theta_0=\frac{\pi}{6}$

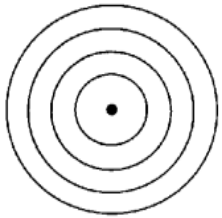

$s=+1, \theta_0=\frac{\pi}{2}$

(+,+) and (-,-) : repulsive
(+,-) : attractive

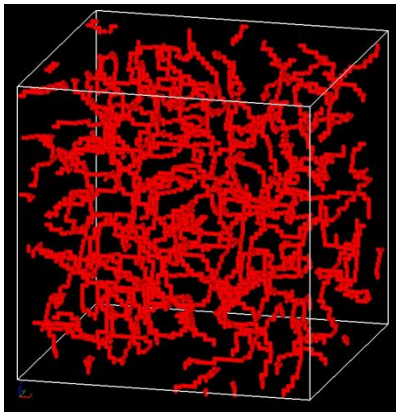

A line defect has a tension in 3D.
It tend to be shrunken.

Annihilation of defects

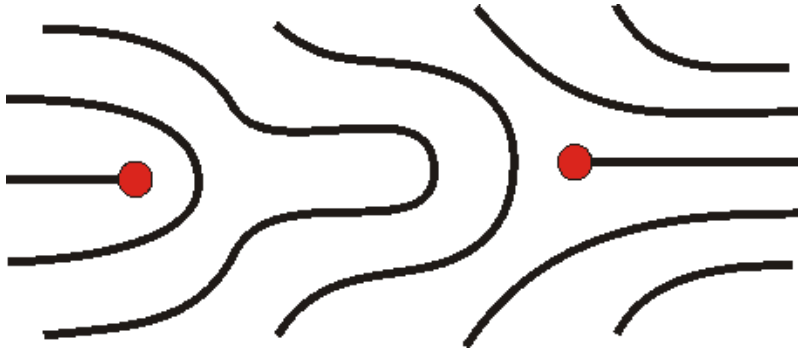

$s = -\frac{1}{2}$ $s = +\frac{1}{2}$

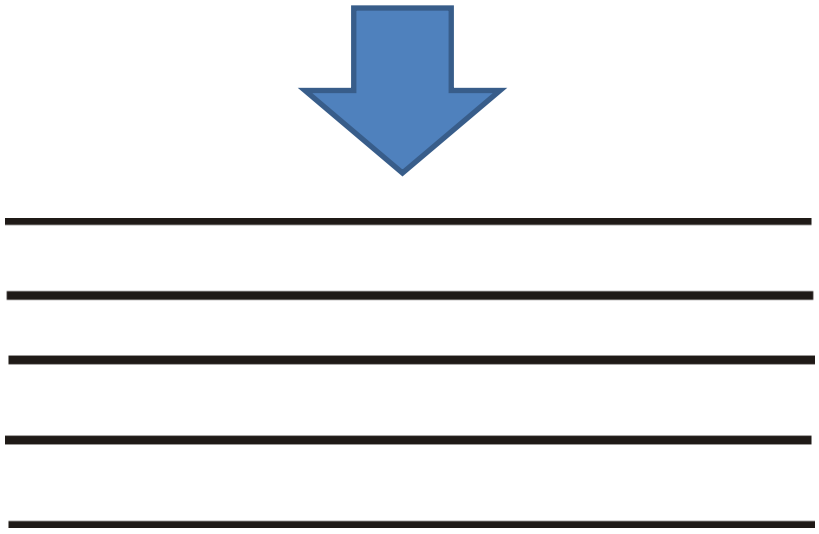

In bulk, defects of nematic phase are not long-lived

A defect of the topological charge S is annihilated with other one of $-S$

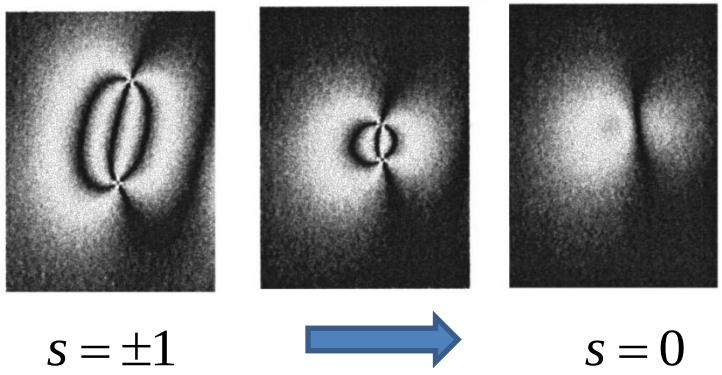

$s = \pm 1$ $s = 0$

Minomura *et al*. (1997)

Re-organizations of defects

TABLE I. Event classification list. The first column gives the identification number we have given each type of event.

Code	Event pictograph	Description
1		Intercommutation of two $\pm\frac{1}{2}$ strings (The two initial strings are separated in space)
2		Decay of a ±1 across two $\pm\frac{1}{2}$'s into two $\pm\frac{1}{2}$'s
3		Decay of two ±1's across two $\pm\frac{1}{2}$'s into two $\pm\frac{1}{2}$'s
4		Intercommutation of a $\pm\frac{1}{2}$ and a ±1 resulting in a $\pm\frac{1}{2}$ with two T intersections
5		Intercommutation of two $\pm\frac{1}{2}$'s resulting in two $\pm\frac{1}{2}$'s connected by a ±1
6	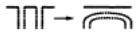	Unlinking of two ±1's from a $\pm\frac{1}{2}$
7	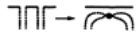	Unlinking of two ±1's from a $\pm\frac{1}{2}$ resulting in a single $\pm\frac{1}{2}$ and a monopole carrying ±1
8		Decay of a ±1 connecting two parts of the same $\pm\frac{1}{2}$ into a single $\pm\frac{1}{2}$
9	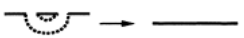	Decay of a ±1 connected at both ends to a straight segment of a $\pm\frac{1}{2}$
10	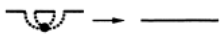	Decay of a monopole carrying ±1 connected at both ends to a straight segment of a $\pm\frac{1}{2}$
11		Decay of a monopole sitting on a ±1 by absorption into a $\pm\frac{1}{2}$
12		Collapse of a $\pm\frac{1}{2}$ loop (no end products)
13		Collapse of a $\pm\frac{1}{2}$ loop with a ±1 across it
14		Collapse of a $\pm\frac{1}{2}$ loop with two ±1's coming out at either end, resulting in a single ±1
15		Collapse of a $\pm\frac{1}{2}$ loop, with two attached ±1's, resulting in a monopole carrying ±1
16		Collapse of a $\pm\frac{1}{2}$ loop with four attached ±1's resulting in a four-(±1) vertex which escapes

Chuang *et al*. (1993)

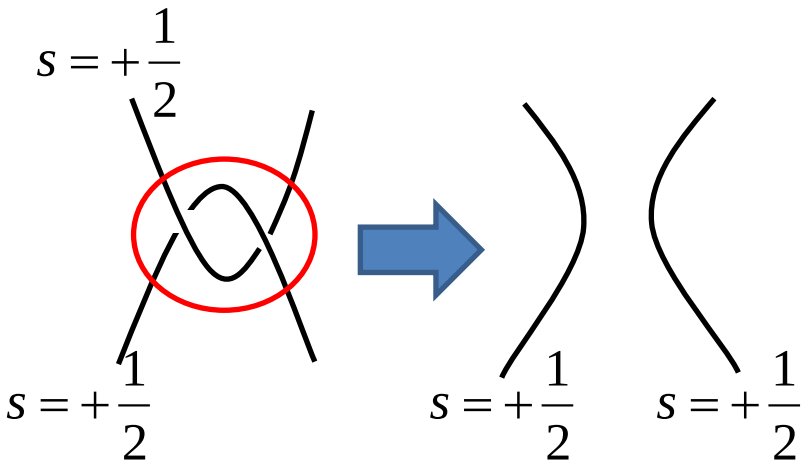

Energy barrier for a reorganization

$$\Delta E \sim K^{3/2}\Delta\mu^{-1/2}$$

K:elastic modulus
$\Delta\mu$: chemical potential difference

Simulations of nematic ordering

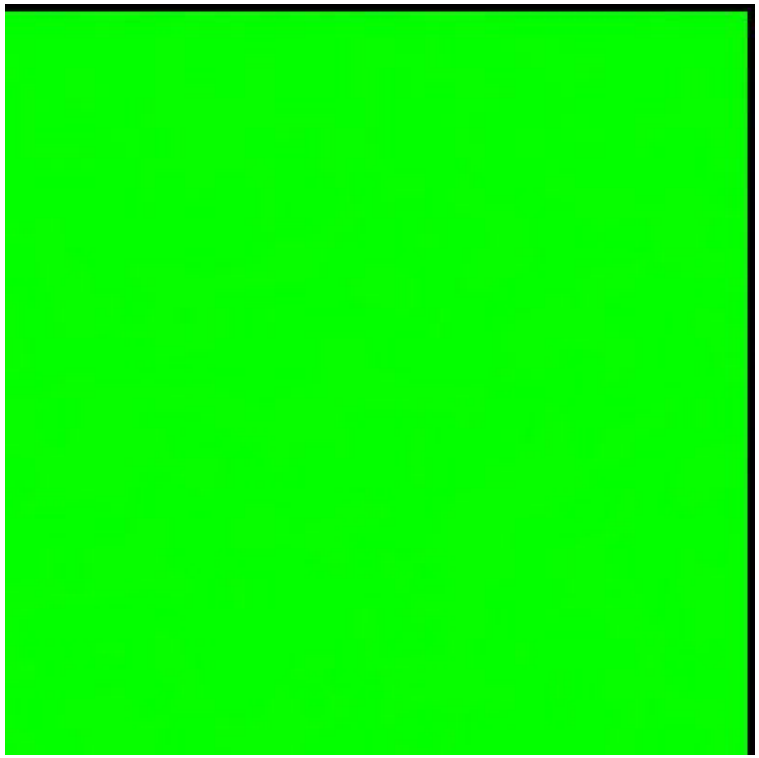

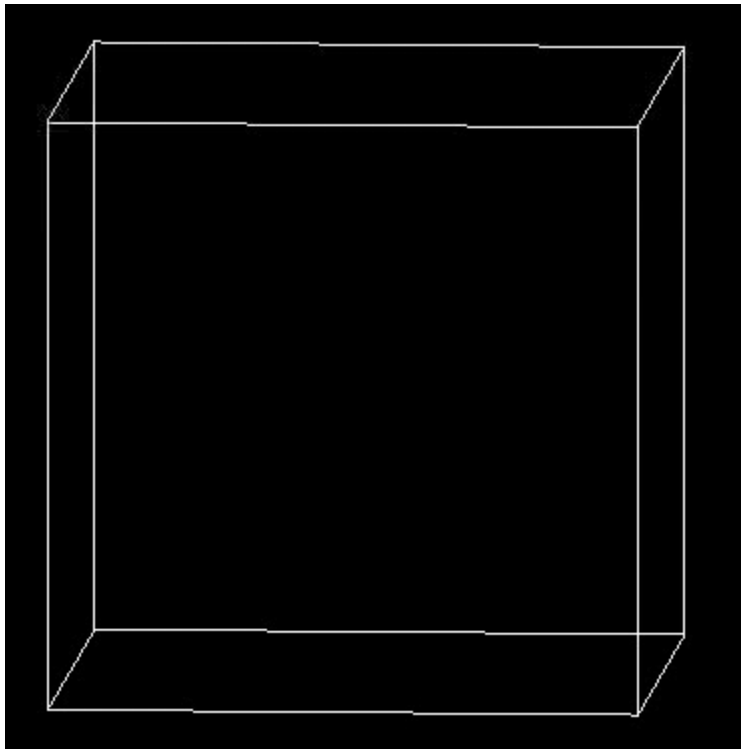

Characteristic length
(Typical separation between defects)

$$R \propto t^{1/2}$$

Anchoring effect

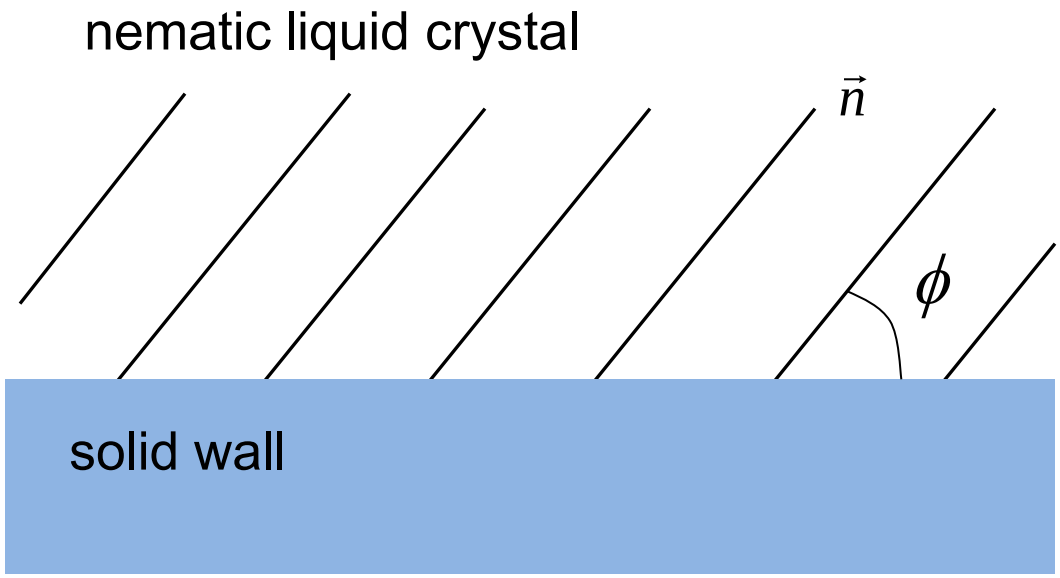

Director field is aligned at solid surface with tilt angle ϕ

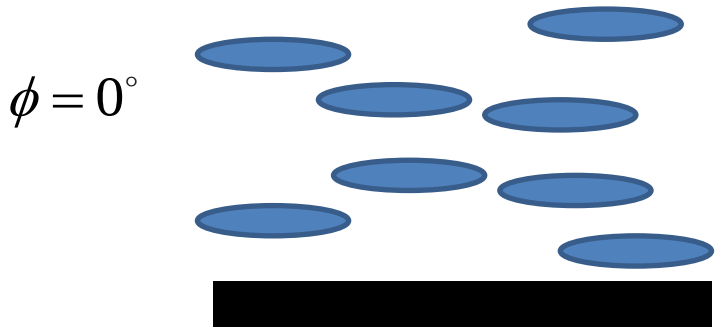

planar

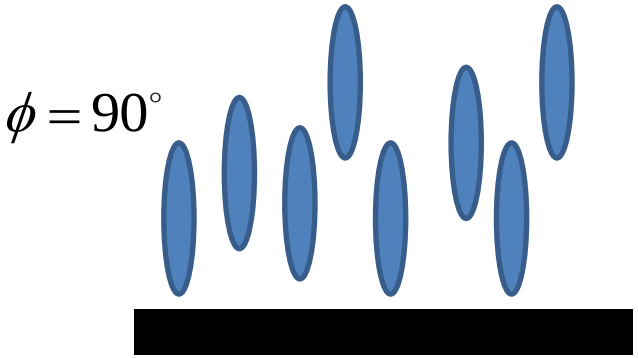

homeotropic

Liquid crystal and solid objects

The inclusion of solid objects imposes the formation of defect in liquid crystals

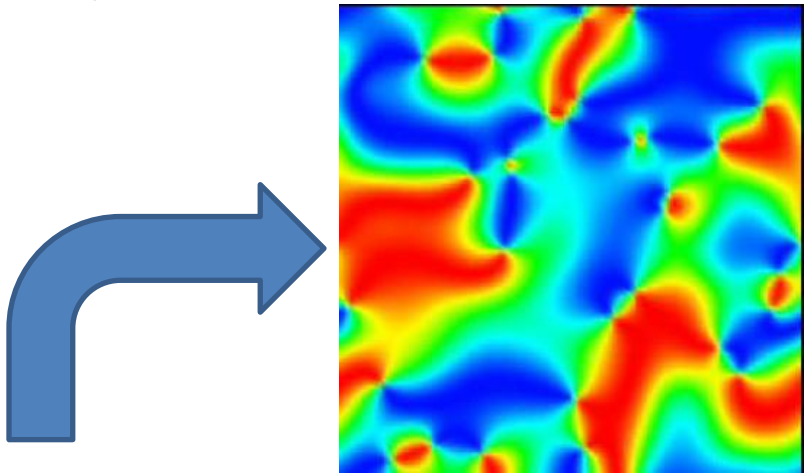

nematic liquid crystal

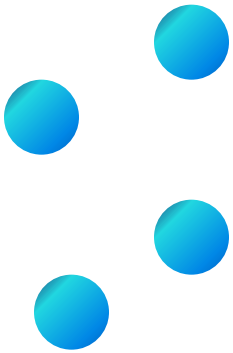

particles (colloids)

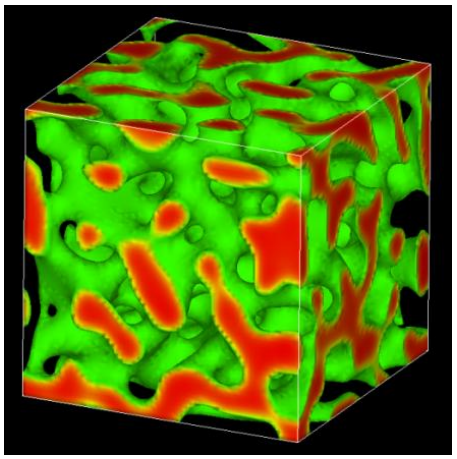

porous media

A particle and defect in NLC

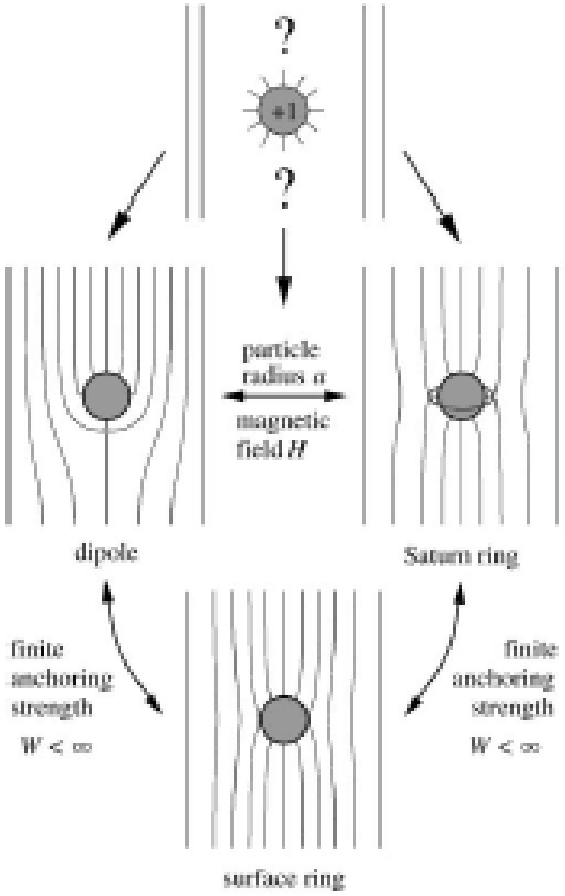

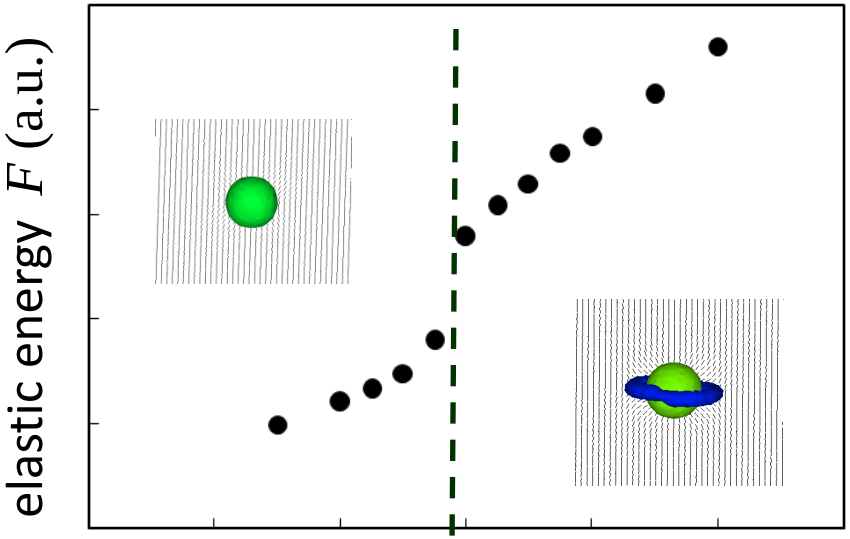

$$W_c = C\frac{K}{a} \quad (C \approx 3.5)$$

H. Stark, Phys. Rep. 351, 387 (2001).

Topology of defect structure

A Saturn-ring defect

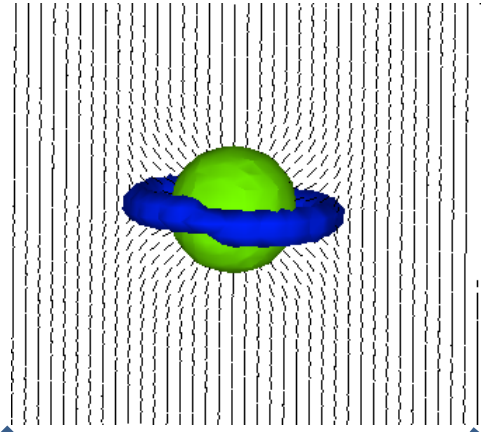

Araki and Tanaka (2006)

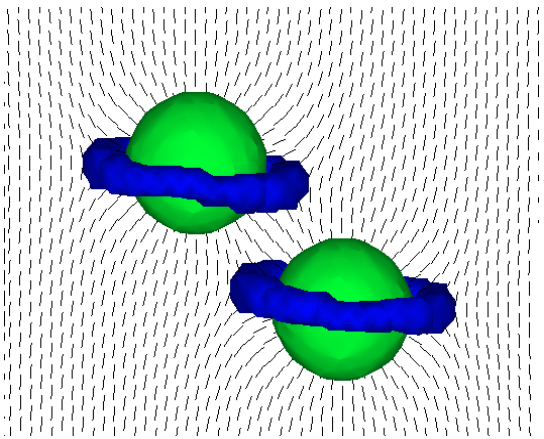

<

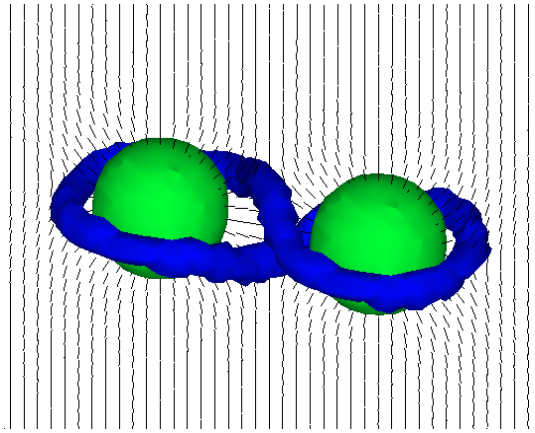

Topologically arrested structure

Aggregation of colloids

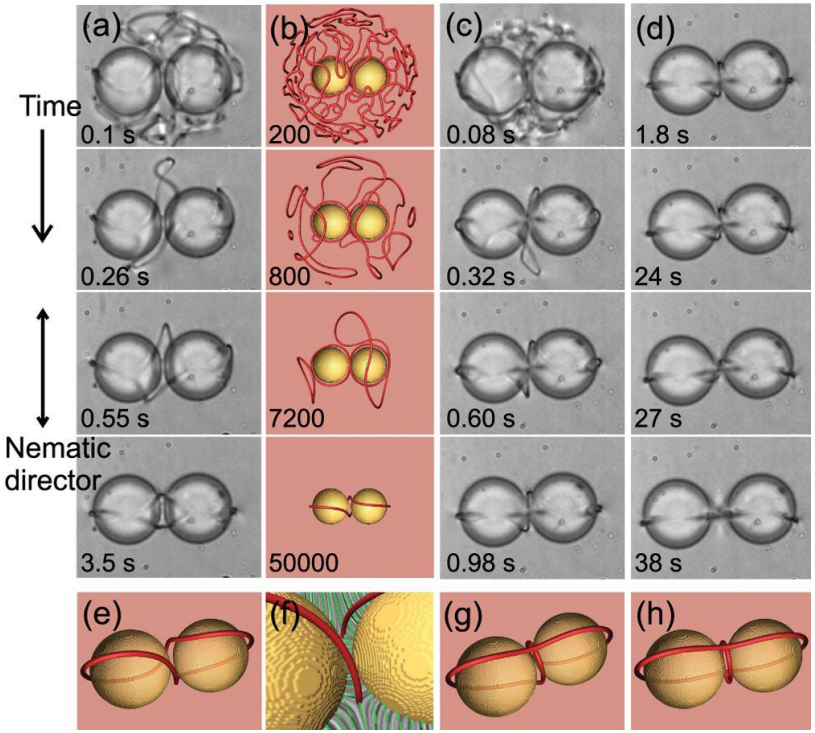

Ravnik et al. (2007)

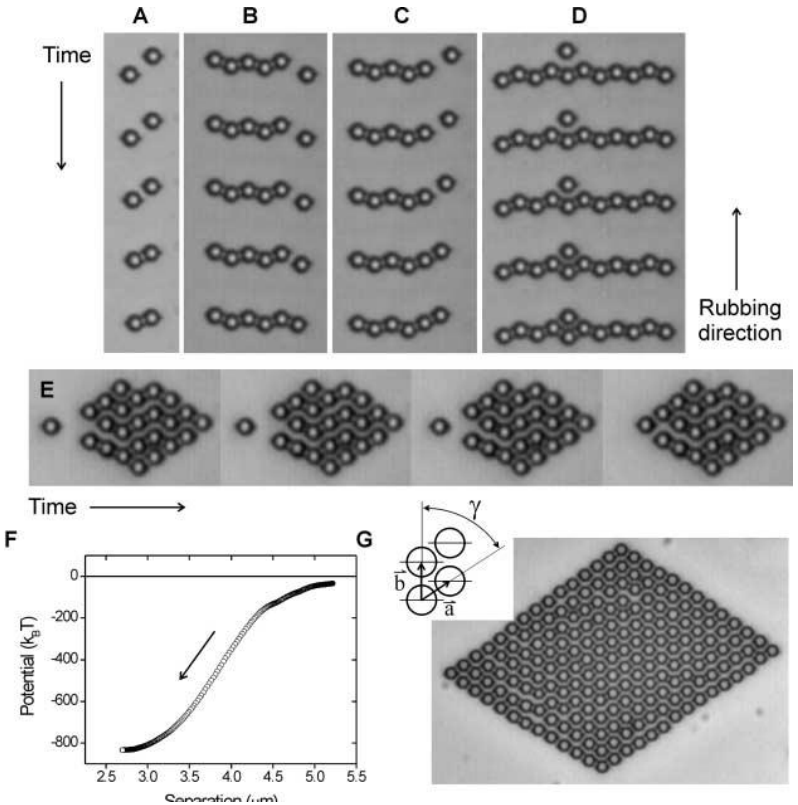

Musevic et al. (2006)

Nematic liquid crystal in porous media

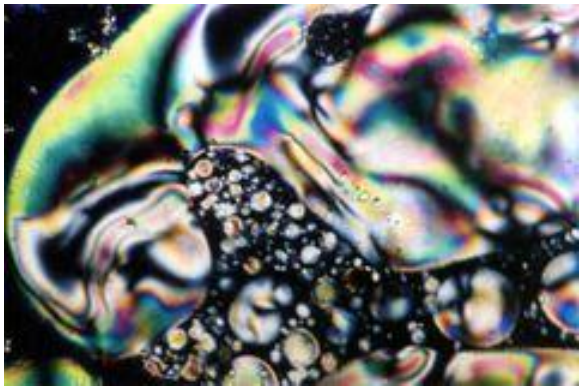

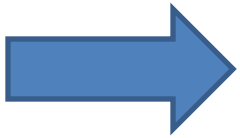

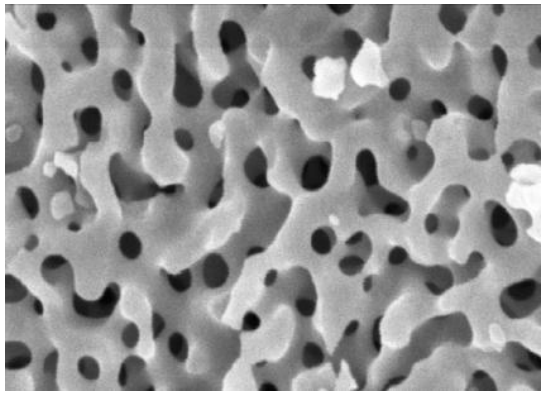

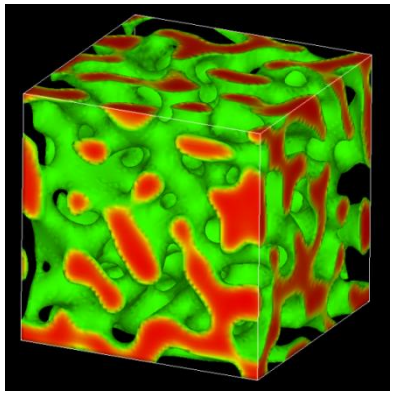

Nematic liquid crystal

porous media(PM)

They show interesting behaviors due to the topological constraints of the defects. And they provide promising properties for optical devices.

(Crawford and Zumer (1996)),
Bellini *et al.* (1996,2000,2002).

Nematic liquid crystal in a simple cell

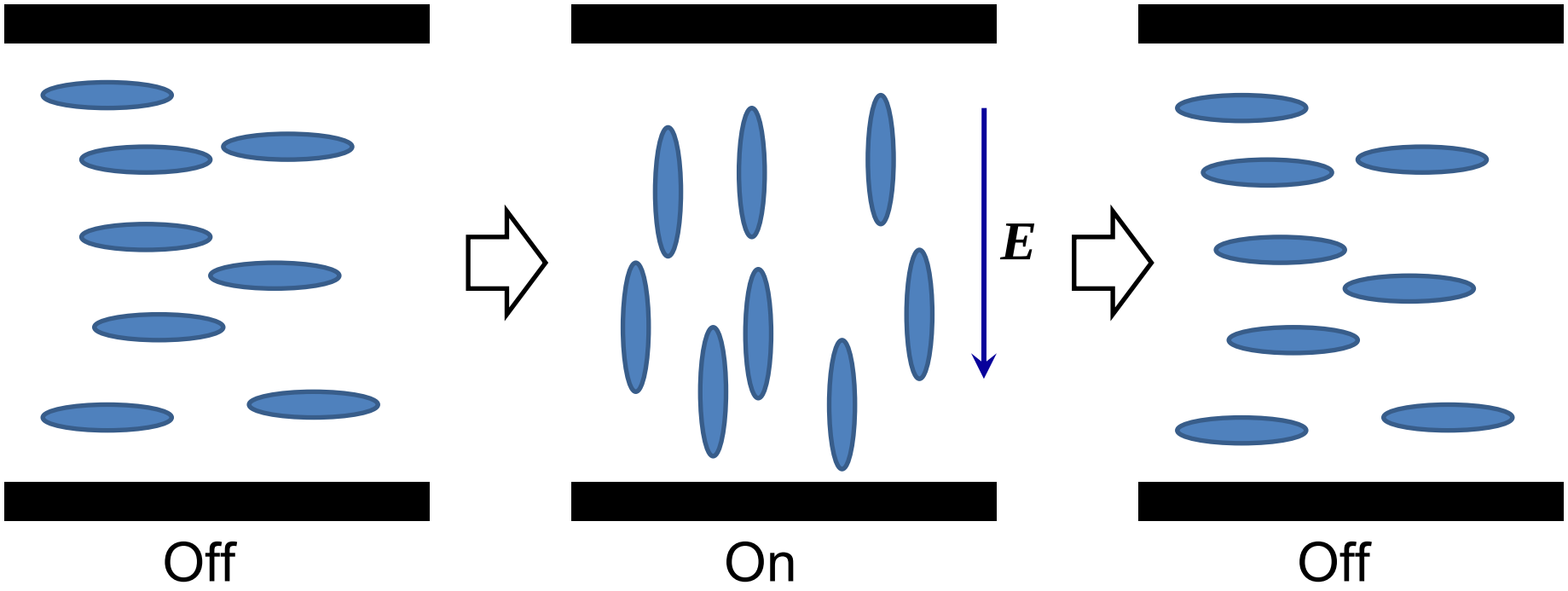

The director field can be tuned by external field.
Soon after the field is switched off, it will recover the original pattern.

Memory effect of confined nematic liquid crystal

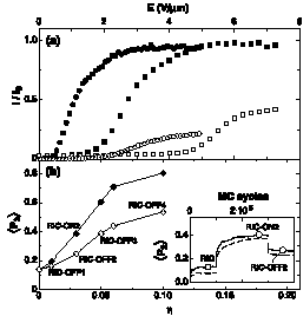

FIG. 1. Comparison between data obtained by optical measurements [Panel (a)] and SSS MC simulations [Panel (b)] in a ZFC experiment: the system is quenched in the N phase with no external electric field applied. After the equilibration an electric pulse is applied and the data are collected in presence (filled symbols) and after the removal (open symbols) of the applied field E. Panel (a) Transmitted intensity normalized to the isotropic value I/I_0 measured as a function of the amplitude of 1 kHz electric field applied for 5 seconds. The samples are thermalized at 10 °C below the I to N transition temperature. Circles: 3 μm Millipore membrane imbibed by 5 CB [11]. Squares: Filled nematic composed by 6 CB and 15% Aerosil [10]. Panel (b) Asymptotic order parameter $\langle P_2 \rangle$ plotted as a function of electric field strength η. Data obtained with a 50^3 cube with $p = 14\%$. Inset: $\langle P_2 \rangle$ plotted as a function of the MC cycles for $L = 50$ (solid line) and $L = 80$ (dashed line). The electric field $\eta = 0.03$ is ON in the MC cycles interval [100 000, 200 000] and OFF elsewhere. In the inset three states are defined: the initial state (zero-FC or RIC), the ON asymptotic state in the presence of a field, and the OFF asymptotic state after the removal of the field. The acronyms in the figures indicate the configurations described in the text and in Table I.

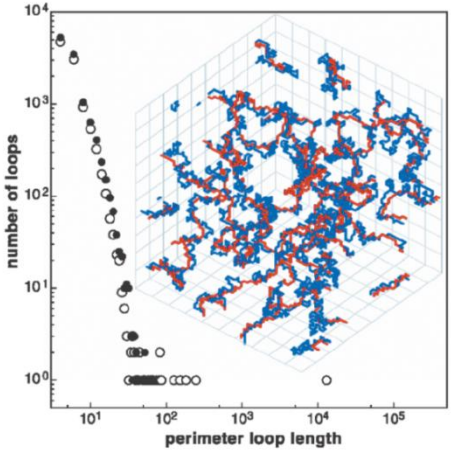

FIG. 2 (color). DL perimeter length distribution for AIC (dots) and RIC (open circles) for $L = 80$ and $p = 0.14$. Inset: snapshot of the longest DL (2968 lattice units) in a RIC state, $p = 0.14$, $L = 50$ (blue line). The red line is the longest DL (1392 lattice units) obtained through the domain freezing procedure applied to the same RIC system (see text for details).

Rotunno *et al*. (2005). Buscaglia (2006)

A nematic liquid crystal in a porous medium can efficiently keep its orientational order, even after the field is switched off.
The nematic liquid crystal memorizes the orientational field.

The aim of this study is to explore the mechanism of the memory effects.

Preparation of random porous media

Cahn-Hilliard-Cook equation

$$\frac{\partial \phi}{\partial t} = \nabla^2\left(-\phi + \phi^3 - \nabla^2\phi\right) + \theta$$

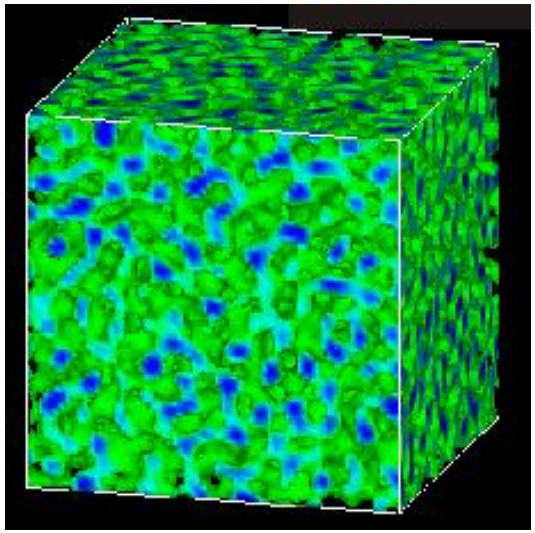

$\ell = 4.6$

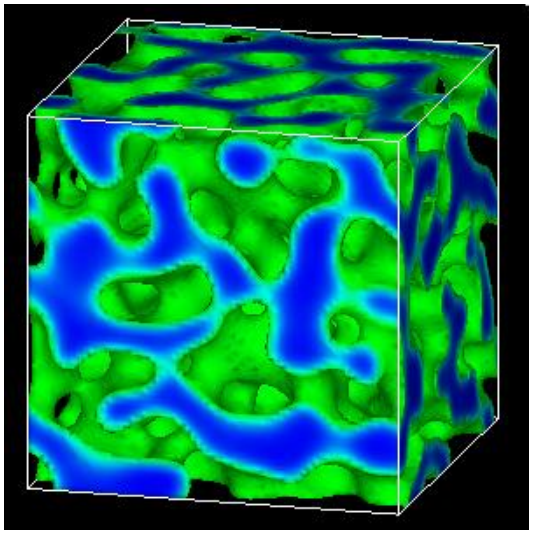

$\ell = 11.8$

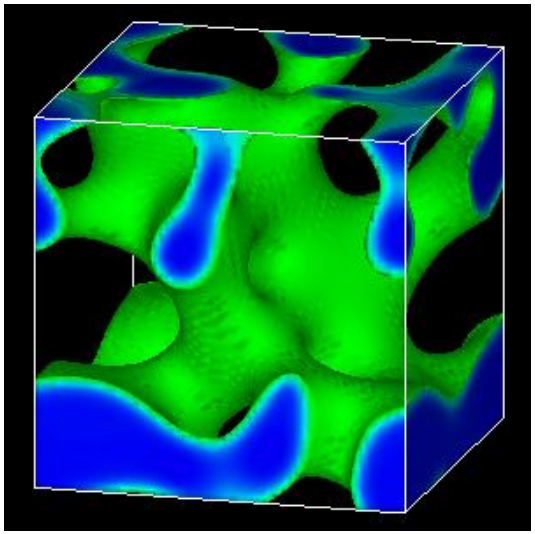

$\ell = 30.7$

We can obtain isotropic random porous media with controlled sizes.

ℓ : mean pore size

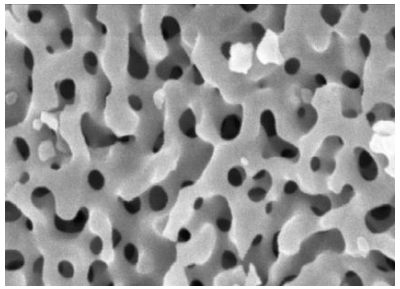

Spatial distributions of Q

Red regions represent the porous medium

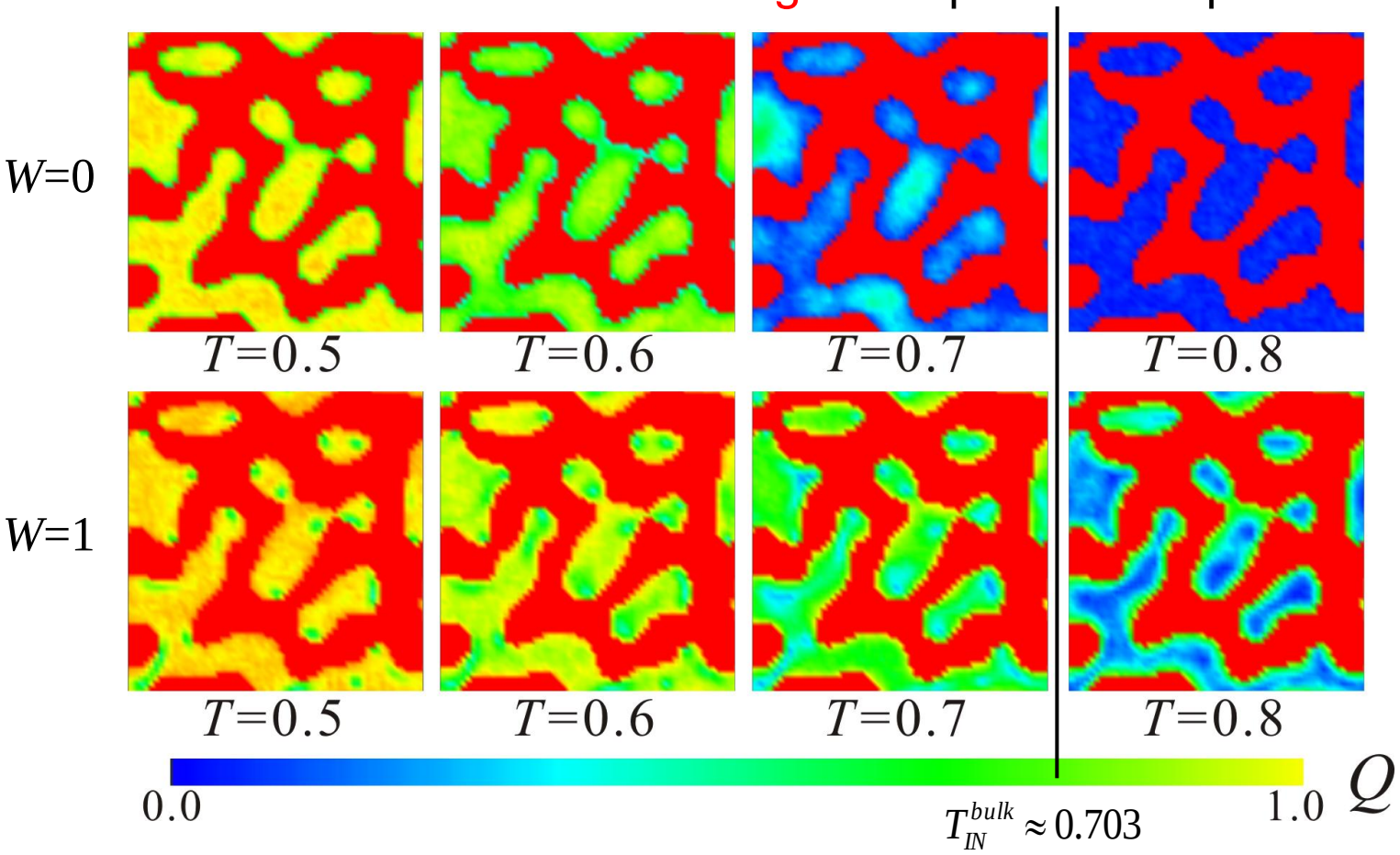

The nematic order grows from the surfaces in a porous medium with finite W.

Defect structure of nematic liquid crystal in porous media

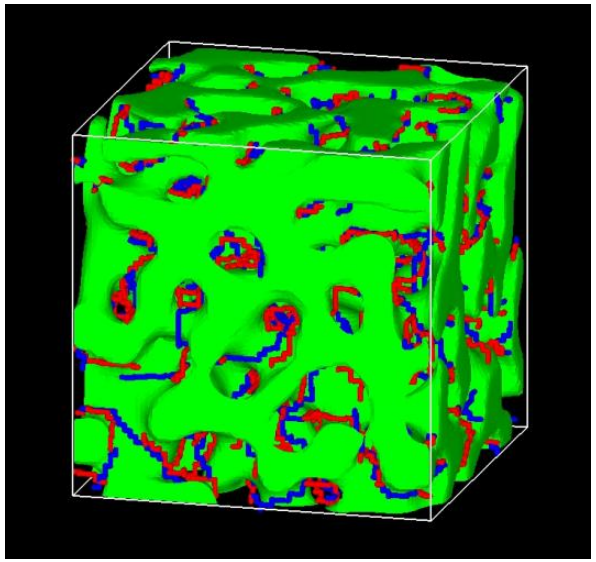

defect structures for different simulations of the same condition

Since all the channels do not necessarily have disclination lines running through them, many metastable configurations can be found.

The defect configurations are long-lived since the energy barriers connecting them are associated to simultaneous liquid crystal rotation in entire channels, and hence larger than thermal fluctuations.

This results in non-ergodic glassy behaviors, analogous to a spin glass.

The number of the possible configurations is estimated as, $(p-1)^{1-\chi/2}$

p average number of arms at nodes, typically $p \approx 3-6$

χ Euler characteristic (topological invariant) $\chi = \frac{1}{2\pi}\int dSK$

~$10^{1000000}$ for 1 mm cell of 1μm pores !

Transformation of defect structure by an external field

E=0.3

E=1.0

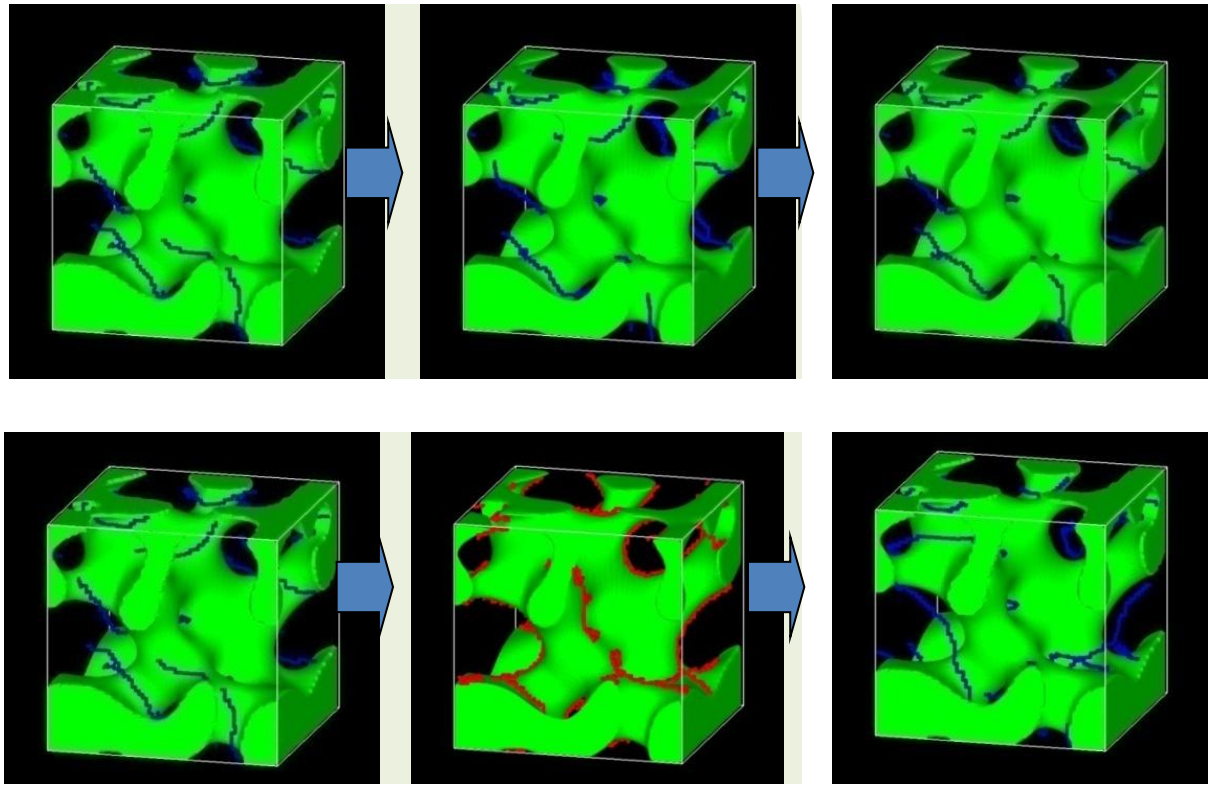

after the quench　under an electric field　after the application

A strong field melts the defect structure and
the topology of defect structure can be changed.
The new topology is conserved even after the field is switched off!

Induced and remnant nematic orders

Orientational order along the field $Q^* = \frac{1}{Q_0(T)}\left\langle \frac{3}{2}\left(n_z n_z - \frac{1}{3} \right) \right\rangle$

simulations

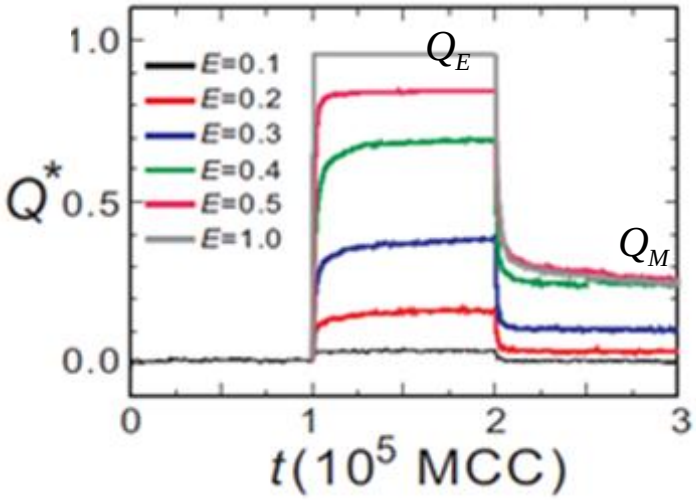

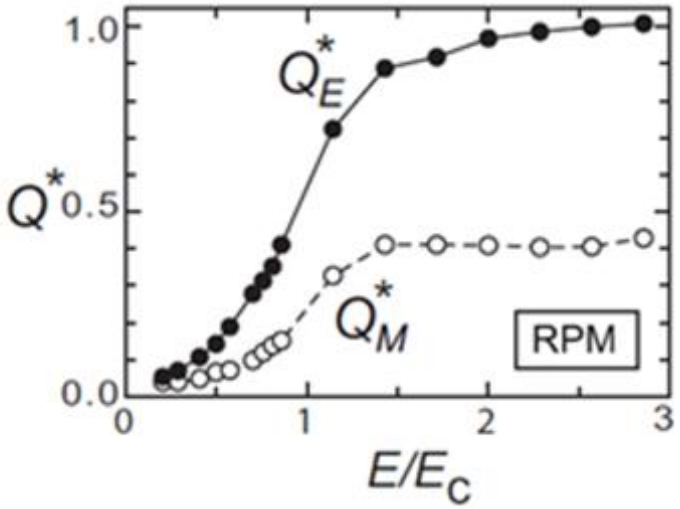

experiments (5CB in millipore filter (3μm) and silica gel (0.8μm))

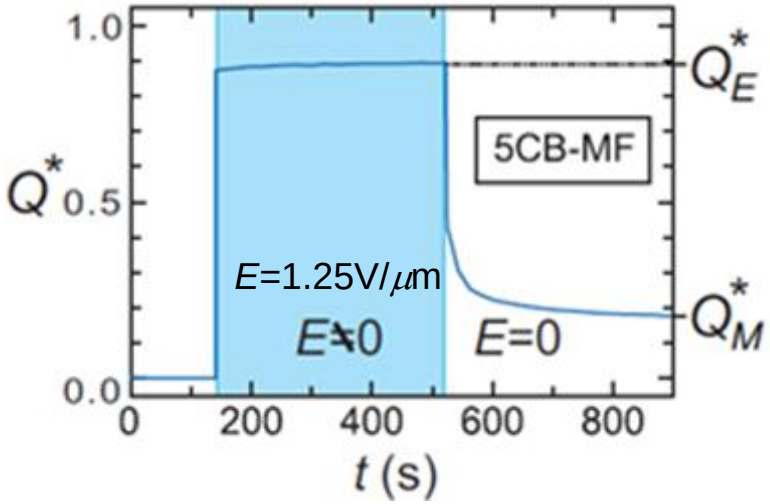

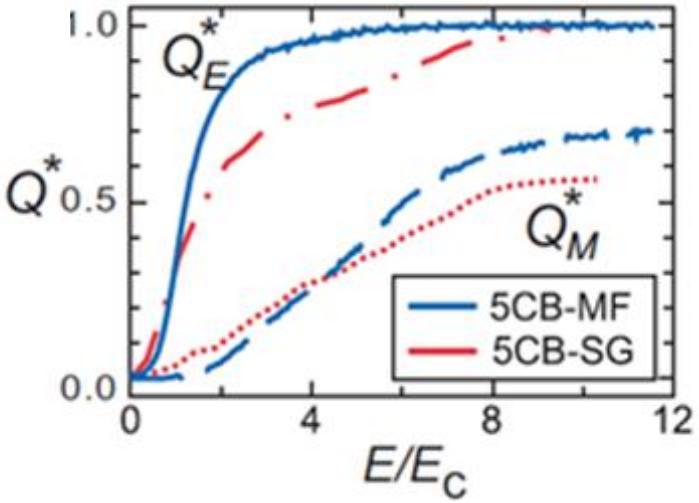

NLC in regular porous materials

Bicontinuous cubic (BC) Simple cubic packing (SC) Cylindrical channels (Cyl)

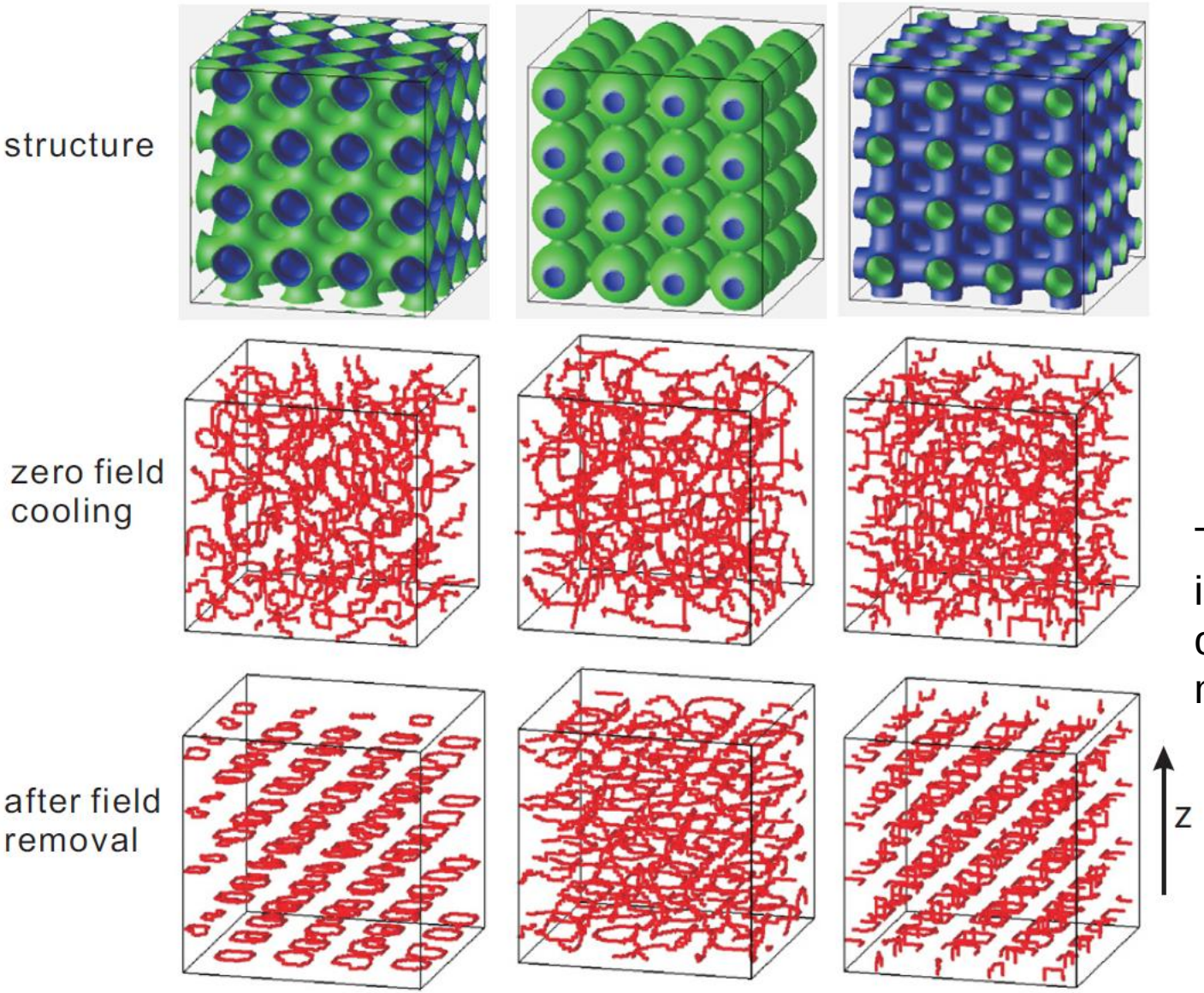

The defect structure is also regular in ordered porous media.

Relaxation of memorized order

Random porous medium (PPM)

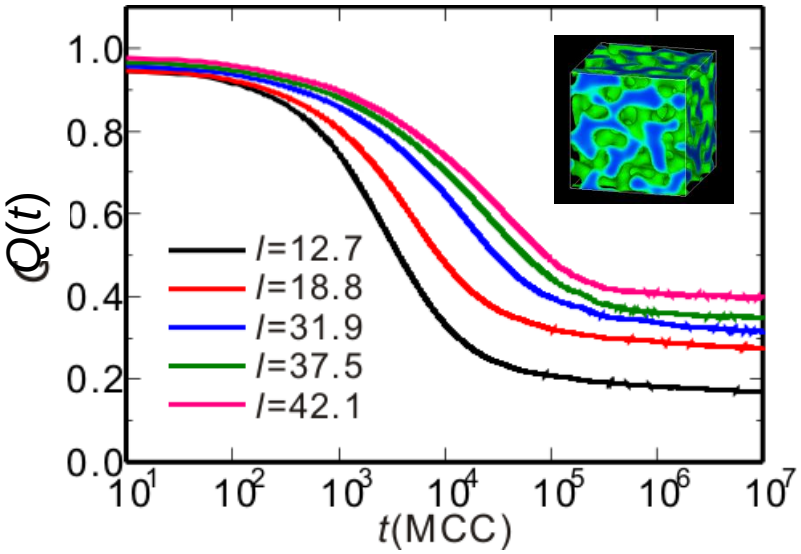

Bicontinuous cubic (BC)

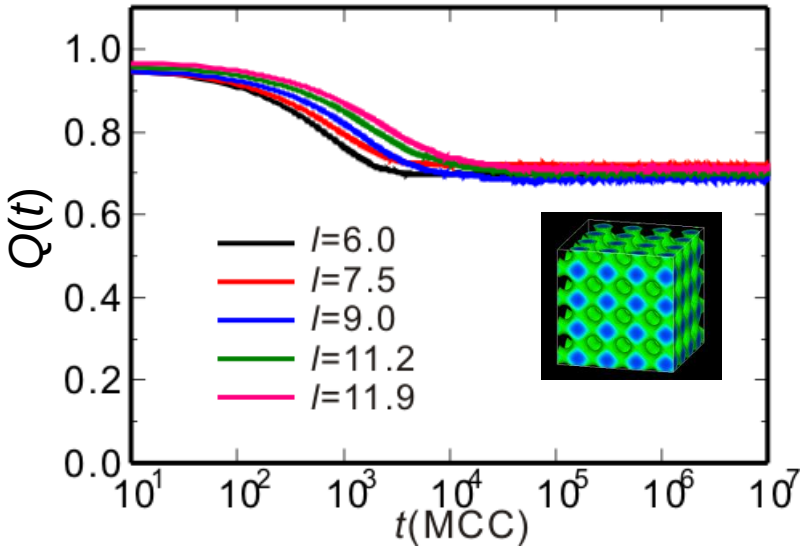

In BC, only a single relaxation mode is observed.
After the fast mode, the second slow relaxation appears in RPM.

BC: single stretched exponential decay

$$Q(t) = Q_M + \Delta Q_S \exp(-(t/\tau_S)^{\alpha})$$

RPM: stretched exponential decay and logarithmic decay

$$Q(t) = Q_M + \Delta Q_S \exp(-(t/\tau_S)^{\alpha}) + \frac{\Delta Q_L}{1+\log(1+t/\tau_L)}$$

Logarithmic decay for superconductor:
Anderson (1962)
Kim *et al.* (1962)

Fast relaxation mode

In the both type of porous media, the fast relaxation mode represents the recovery of the elasticity of the nematic phase that is distorted by the external field.

In this fast process, the topology of the defect structure does not change.

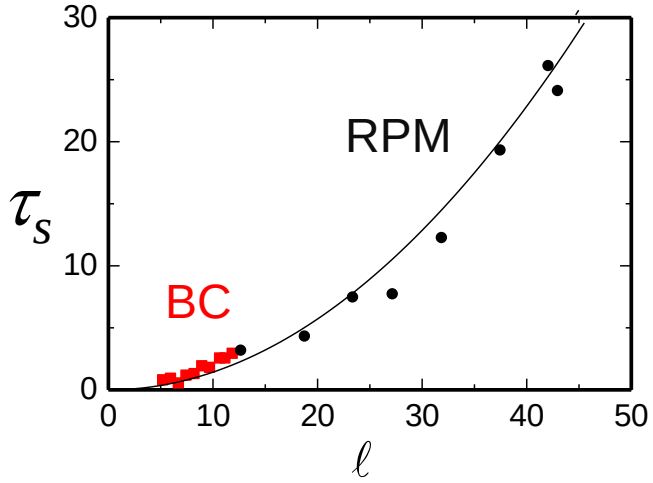

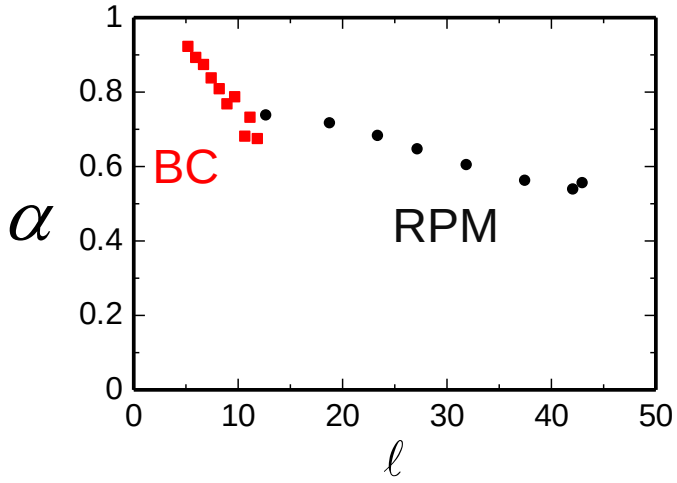

The elastic theory predicts the relaxation time is proportional to l^2 in the limit of the strong anchoring.

$$F\{\vec{n}\} = \frac{1}{2}K\int dV\left|\nabla\vec{n}\right|^2 - W\int dS\left(\vec{n}\cdot\vec{s}\right)^2$$

$$\frac{\partial}{\partial t}\vec{n} = -\frac{1}{\nu}\frac{\delta F}{\delta\vec{n}}$$

$$\tau_S = \frac{\nu\ell^2}{K}$$

T-Dependence of the relaxations

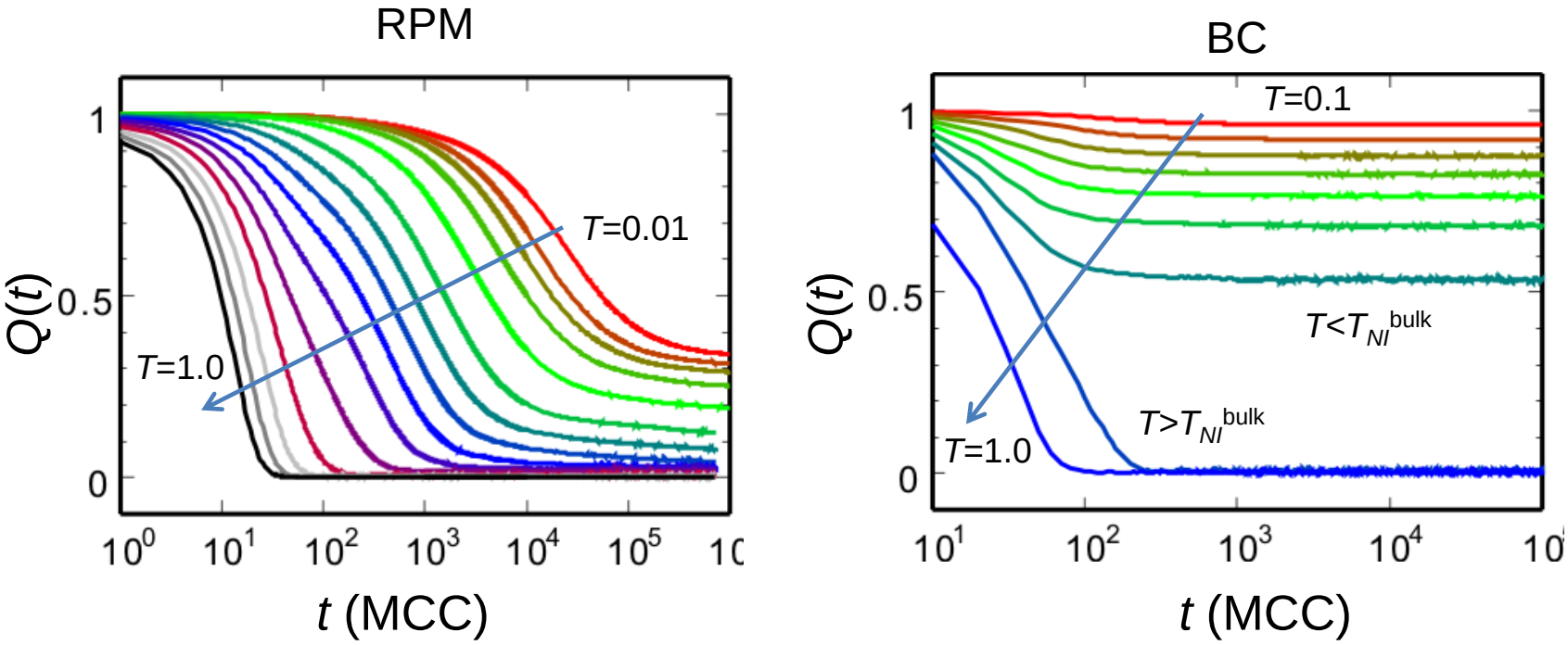

In BC, the remnant order is almost proportional to the bulk nematic order. Above T_{NI}^{bulk} , it decays to zero without the slow mode.

In RPM, the second mode becomes slower with decreasing temperature.

What is the mechanism of the second mode in RPM?

The topological change of the defect structure in RPM

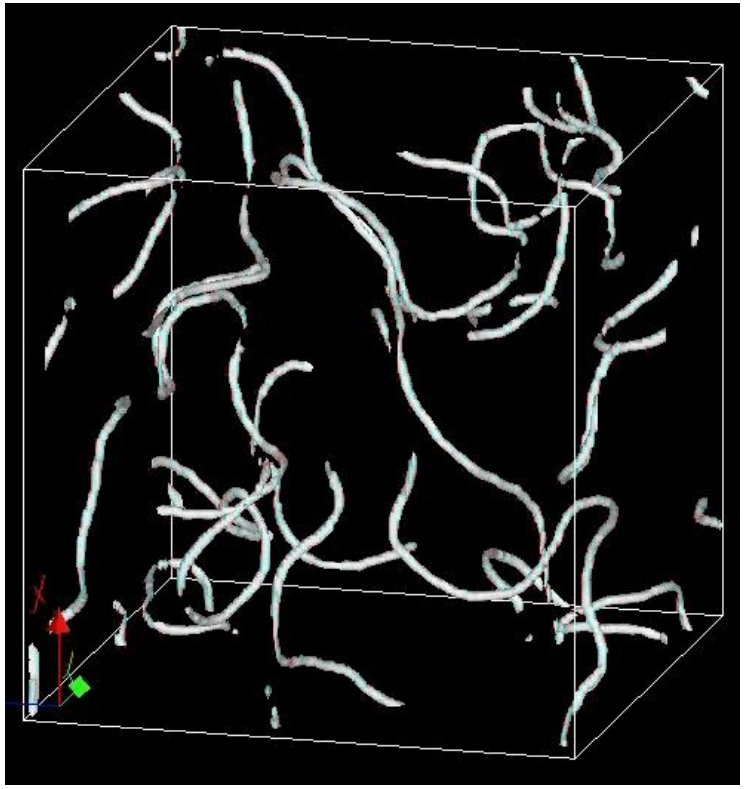

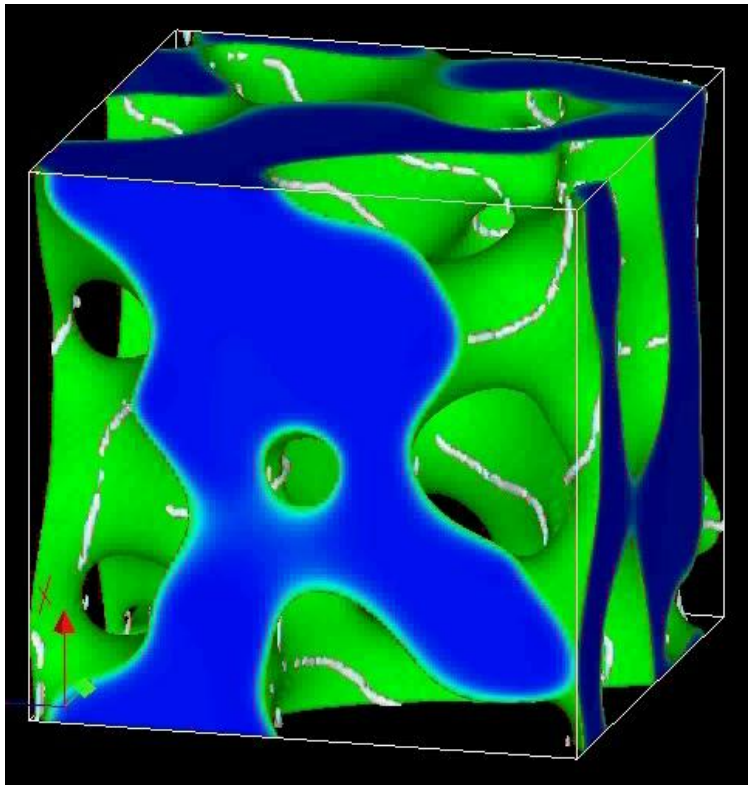

At T=0.1 for $\ell = 43.9$

The second slow mode stems from the reorganizations of topology of the defect structure

The second slow relaxation in RPM

$$Q(t) = Q_M + \Delta Q_S \exp(-(t/\tau_S)^{\alpha}) + \frac{\Delta Q_L}{1+\log(1+t/\tau_L)}$$

Pore size ℓ -dependence at T=0.1

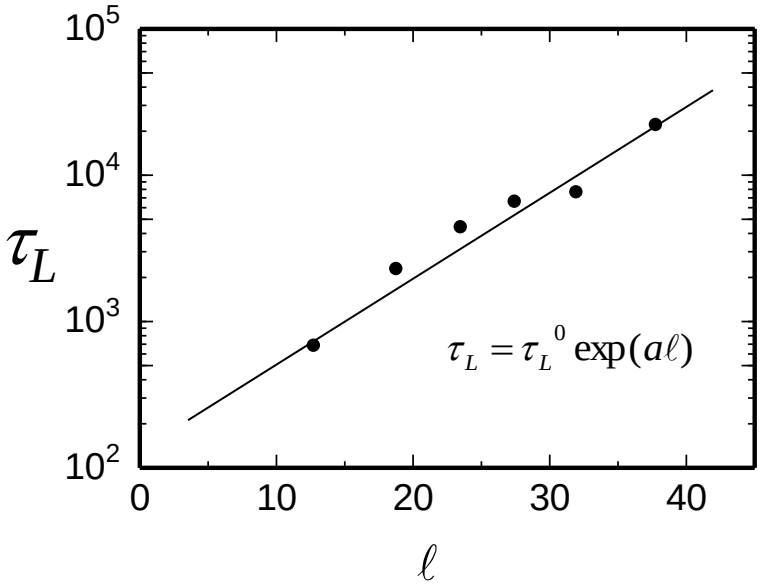

Temperature dependence for $\ell = 12.7$

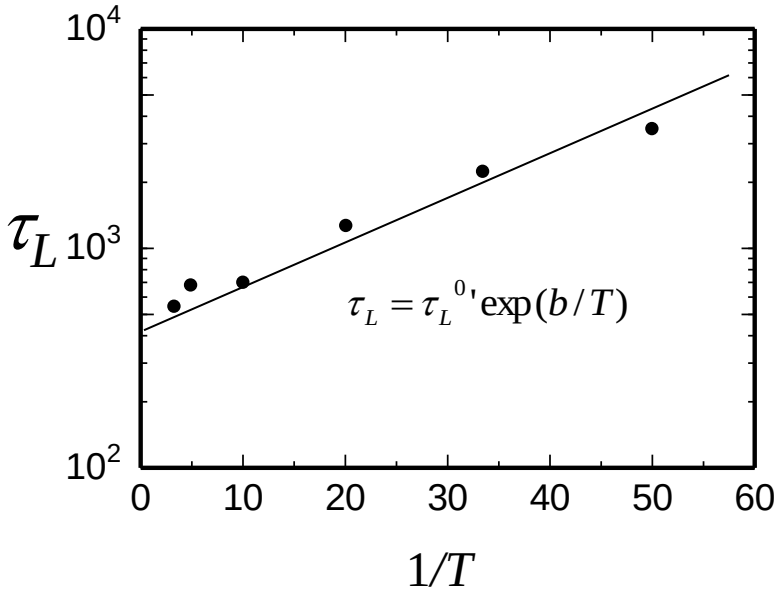

$$\ln \tau_L \propto \ell / T$$

In BC, the defect structure reaches the more stable configuration after the fast mode. Then, the second mode is absent.

The topological change of the defect structure in RPM

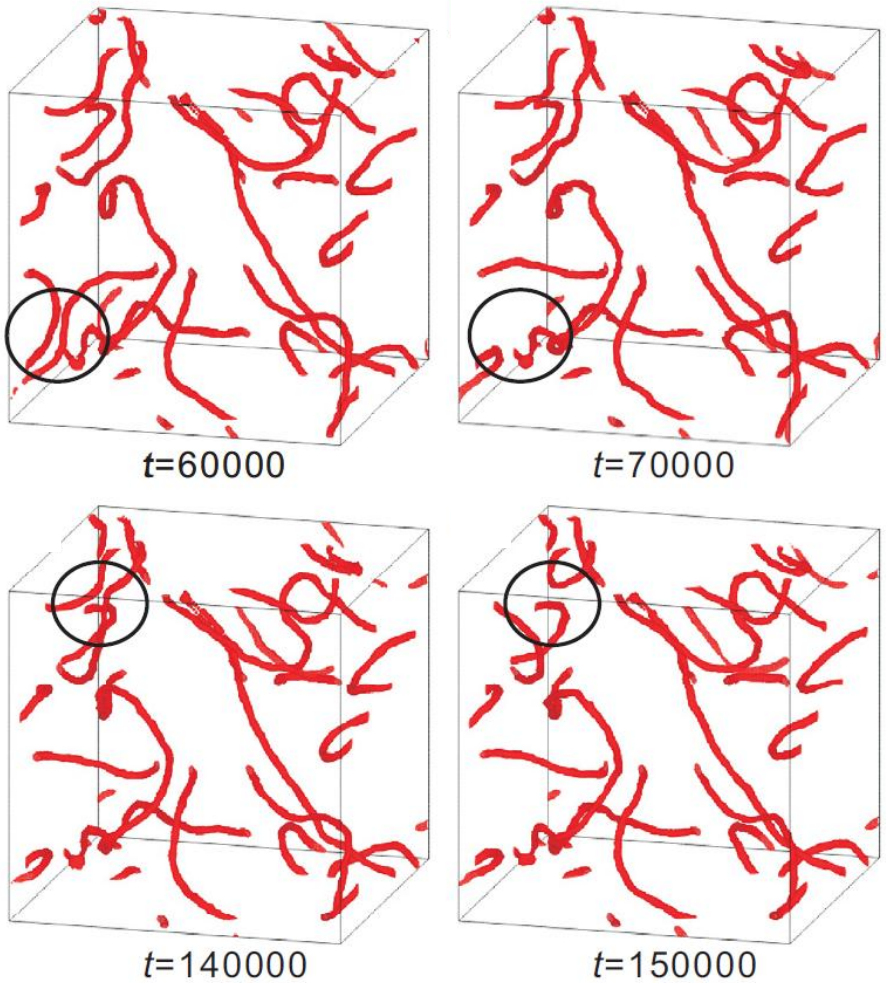

In a subunit of the volume ℓ^3, the elastic energy density is estimated as

$$e = \frac{1}{2} K (\nabla \vec{n})^2 \sim \frac{1}{2} \frac{K}{\ell^2}$$

Thus, the stored elastic energy in this small volume is

$$E = e\ell^3 \propto K\ell$$

The energy barrier against the topological change is also scaled as $K\ell$

$$\tau_L \propto \exp(cK\ell / T)$$

T and *l* - dependences of the remnant orders

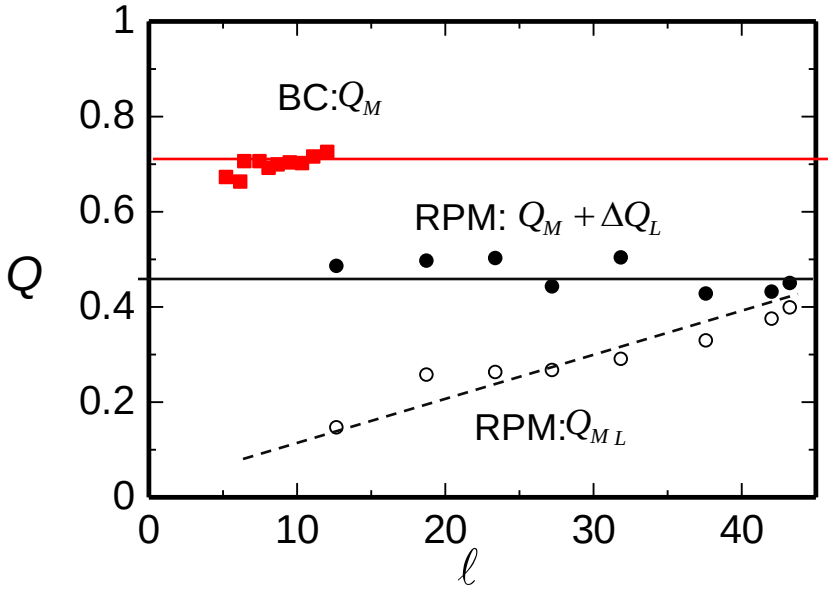

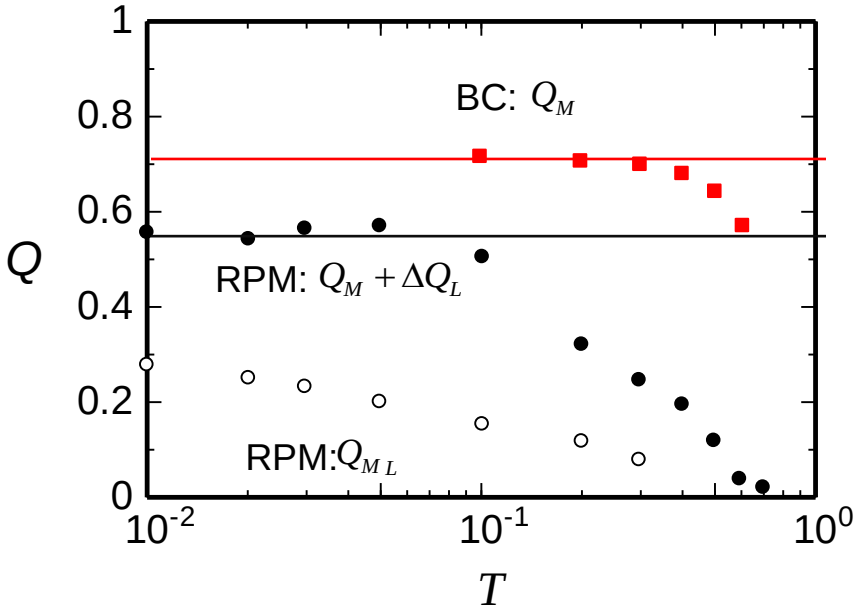

BC: $Q(t) = Q_M + \Delta Q_S \exp(-(t/\tau_S)^{\alpha})$

RPM: $Q(t) = Q_M + \Delta Q_S \exp(-(t/\tau_S)^{\alpha}) + \dfrac{\Delta Q_L}{1+\log(1+t/\tau_L)}$

In BC, the remnant order appears to be independent of the pore size. This is consistent with the scaling argument for the strong anchoring case.

In RPM, the remnant depends on the mean pore size because of its non-ergodic glassy behavior.

Memory effect of nematic liquid crystal in porous media

bicontinuous cubic

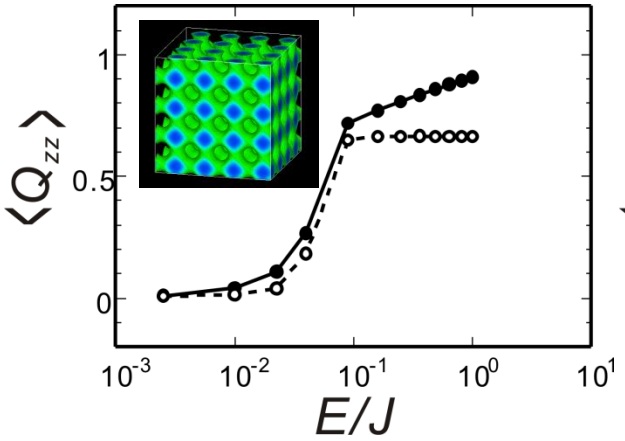

SC sphere array

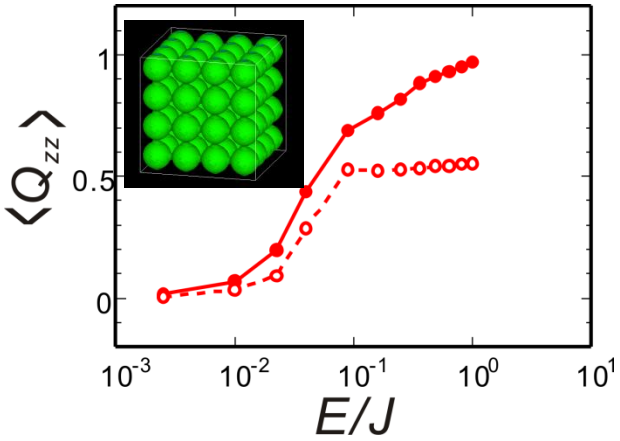

inverted FCC sphere array

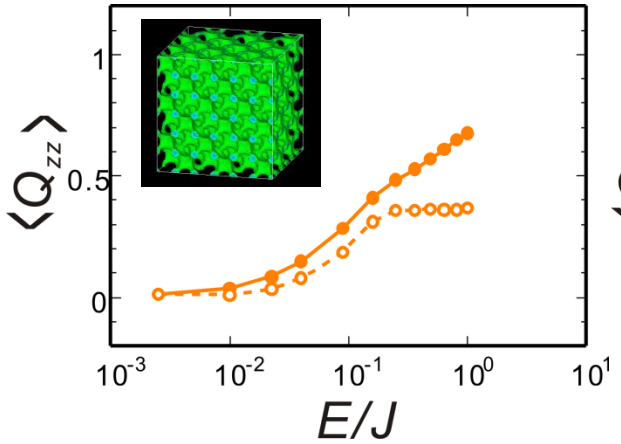

random pores

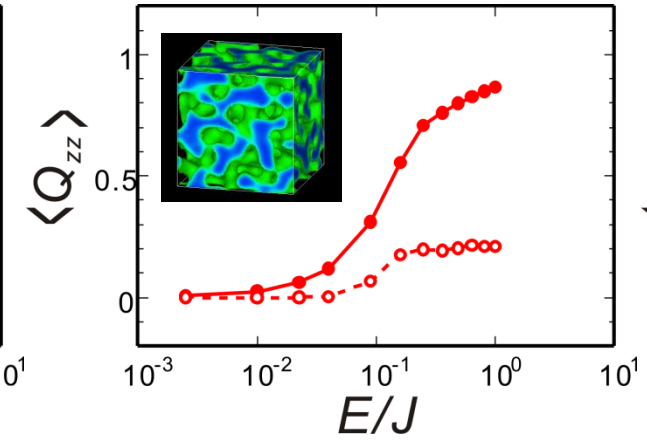

FCC sphere array

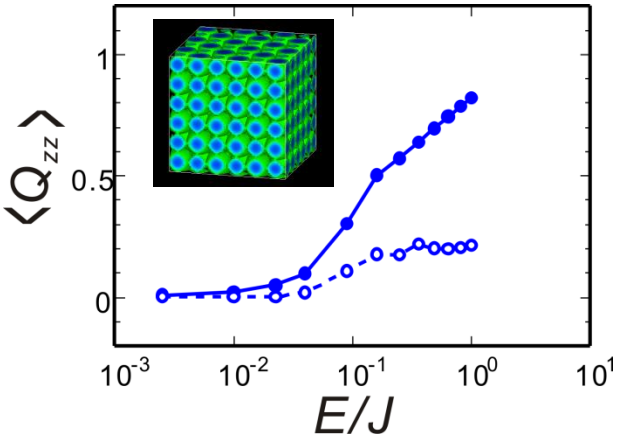

Summary

We numerically studied the glassy behaviors of nematic liquid crystals confined in porous materials.

We found the nematic liquid crystal in porous media shows the two relaxation processes after the external field is removed.

The fast mode represents the viscoelastic relaxation of the director field with keeping the topology of the defect structure.
The second slow one comes from the topological changes of the defect structure toward a more stable configuration.

We also found the remnant order depends upon the pattern of the porous media. By utilizing regular porous media, the second relaxation mode can be controlled.